ОБЪЕДИНЕННЫЙ
ИНСТИТУТ
ЯДЕРНЫХ
ИССЛЕДОВАНИЙ

Дубна

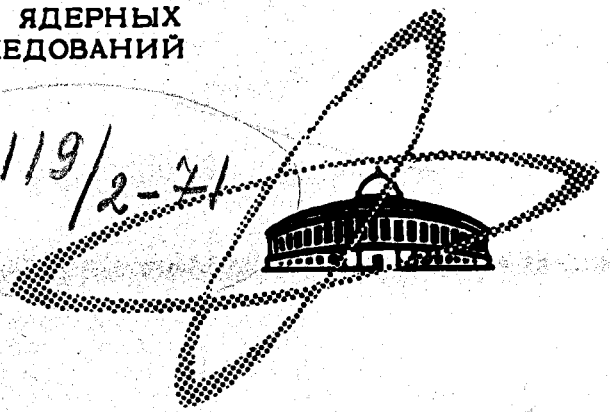

E1 - 5935

B.A. Shahbazian, A.A. Timonina

A SEARCH FOR RESONANCES OF B=2,3 AND S=0, -1, -2

ЛАБОРАТОРИЯ ВЫСОКИХ ЭНЕРГИЙ

1971

E1 - 5935

B.A. Shahbazian, A.A. Timonina

A SEARCH FOR RESONANCES OF B=2,3 AND S=0, -1, -2

Submitted *to* ***Nuclear Physics***

Introduction

A search for resonances of baryonic numbers $B \geq 1$ and strangeness quantum numbers $S = 0, -1, -2$ was carried out. For this purpose the effective mass spectra of the $(pp)-$, $(\Lambda p)-$, $(\Lambda pp)-$ and $(\Lambda\Lambda)$ systems were studied in neutron-carbon interactions at $\langle p \rangle = 7.5$ GeV/c and in π^--carbon interactions at 4.0 GeV/C using the 55cm JINR propane bubble chamber. The neutron beam intensity was 20 and the pion beam intensity was 10 particles per pulse. 150K and 120K photographs were taken, respectively.

Protons were possible to be identified by ionization in this experiment up to 1.0 GeV/c. 80% of protons stopped in the bubble chamber volume. Each event was twice measured and was accepted only when the momenta coincided within one s.d.

Λ-hyperons were identified using the 3C-fit procedure, ionization and δ-electron measurements when the V^0-decay positive particle momentum did not exeed 1.0 GeV/c.

The detection efficiency and its reciprocal - the weight of an event with a V^0-particle - were computed according to the

procedure developed in [1]. All the distributions and effective mass spectra were corrected for the detection efficiency for each event.

1. $B = 2$; $S = -1, 0$ Systems.

Let us at first consider the (Λp) system.

1548 selected neutron-carbon nuclei interactions were subdivided in the following way.

a) 204 were referred to as proton-like events, i.e. baryonic number and the electric charge of the final state systems satisfied the neutron-proton interaction requirements ($B=2$; $Q = +1$), but they failed to fit kinematically (3 C - and $0C$ -fits) the reaction channels

$$np \to p \Lambda K^0 (m\pi^0)$$

$$\to p \pi^+ \pi^- \Lambda K (m\pi^0), \; pK^+ \pi^- \Lambda (m \pi^0) \qquad m = 0,1,2,...$$

$$\to p\pi^+ \pi^+ \pi^- \pi^- \Lambda K^0 (m\pi^0), \; pK^+ \pi^+ \pi^- \pi^- \Lambda (m\pi^0)$$

for one-, three- and five-prong events, respectively. But all these events satisfy the enough, but not necessary criterion that they were created in peripheral collisions of neutrons with carbon nuclei [2].

The corresponding (Λp) effective mass spectrum is presented in Fig. 1a.

b) 602 were one-proton carbon-like events ($B = 2$, $Q = 1$). The effective mass spectrum of all one-proton events (806 in total) is shown in Fig. 1b.

The background, computed in the impulse approximation and normalized to the total weight of 806 events by the dotted hystogram, is presented.

The following scheme is meant by the impulse approximation. Let us consider neutron-carbon interactions resulting in, for example, three-prong proton-like events:

$$
\begin{aligned}
n^1_0\ {}_6C^{12}_6 &\to p\,\pi^+\pi^-\Lambda\,K^0\ {}_5B^{11}_6\ (m\,\pi^0)\\
&\to p\,\pi^+\pi^-\Lambda\,K^0\ n\ {}_5B^{10}_5\ (m\pi^0) \qquad m=0,1,2,\ldots,\\
&\to p\,\pi^+\pi^-\Lambda\,K^0\,3n\ {}_5B^{8}_3
\end{aligned}
\qquad (1)
$$

or the same reactions (1) with the substitution of K^0 and π^+ for a K^+-meson.

Any of these proton-like final states with stable boron isotope nuclei can be formed not only in a single neutron-nucleon collision, but also in different collisions of a nuclear cascade in the same carbon nucleus. For example, the second of the final states (1) can be formed in the following cascade processes:

$$
n^1_0\ {}_6C^{12}_6 \to \pi^+\pi^-\Lambda\,K^0\,n\ {}_6C^{11}_5
$$
$$
\left.\begin{matrix} n \\ \Lambda \\ K \\ \pi \end{matrix}\right\}\ {}_6C^{11}_5 \to p\pi^+\pi^-\Lambda\,K^0\ n\ {}_5B^{10}_5\ (m\pi^0),
$$

etc. This circumstance gives us an opportunity to try to model the observed (Λp) effective mass spectrum using the experimental data. Then three-prong proton-like events are modelled by combining protons from real three-prong proton-like events with real two-prong events created in the reactions: $n^1_0\ {}_6C^{12}_6 \to \pi^+\pi^-\Lambda\,K^0\ {}_6C^{12}_6\ (m\pi^0)$.

The Λ-hyperon momenta and their polar angles of emission were selected in order to make coincide the corresponding distributions with those for Λ-hyperons from real three-prong proton-like events. Then effective masses of all modelled (2438) Λp combinations were computed. Each combination was compared with the enough, but not necessary criterion that the interaction did not take place on a free or a quasi-free nucleon, but that it took place in peripheral interactions of neutrons with carbon nuclei. After the application of this procedure (i.e. after treating the modelled events as real ones) 1232 modelled combinations (events) survived (total weight 2182.31).

The scheme used satisfying all conditions of impulse approximation is at the same time free of various assumptions on nuclear structure and wave functions.

The use of any nuclear model (based, for example, on the Hülten or oscillatory potential) needs for corrections for all possible interactions of primary and secondary particles with nucleons of carbon nuclei as well as with each others and the formation and decay of all known resonances. Besides, one must correct for all experimental biases as, for example, the identification efficiency of charged particles in the function of their momenta, dip angles and chamber illumination conditions, etc., which need for many series of special calibration experiments some of which are not accessible once the exposure is achieved. In contrast, the experimental way proposed solves all these problems automatically.

The modelled (Λp) effective mass spectrum obviously does not contain (Λp) resonating pairs because Λ - hyperons and protons are taken from different events of different classes.

The same procedure can be extended on interactions with more than one proton in the final state. It is obvious that the modelled (Λp) effective mass spectrum should be flatter than for one-proton final states because of the wider (Λp) opening angle distribution in two- and more-proton states.

An additional investigation has shown that the (Λp) opening angle distribution is wider and the (Λp) effective mass spectrum is flatter than the corresponding distribution derived in the frame of our impulse approximation if the Hülten potential model for carbon nucleus is used and protons are treated as spectators.

All these arguments prove that the (Λp) effective mass spectrum obtained in the frame of our impulse approximation gives the realistic and at the same time maximum of all possible backgrounds.

c) The rest of 742 events were of the following topologies:

$2p\Lambda$ - 490 events

$3p\Lambda$ - 195

$4p\Lambda$ - 41

$5p\Lambda$ - 16

The summary (Λp) effective mass spectrum is shown in Figs. 1c, 1d.

Three statistically significant peaks (more than 4 s.d.) are clearly seen at 2058 MeV, 2127 MeV and 2252 MeV (Figs. 1b and 1c).

The one-proton (Λp) mass spectrum with the extracted background is shown in the right upper corner of Fig. 1.

The existence of these peaks in the second experiment with $\pi^- C^{12}$ interactions at 4.0 GeV/C was further confirmed.

586 events with a Λ-hyperon and (1 ÷ 5) protons (the average proton multiplicity was 1.5) were selected. The corresponding (Λp) effective mass spectrum is shown in Fig. 2.

Besides, the fact itself of the observation of the same peaks irrespective of the bombarding particle nature probably indicates the same nuclear cluster nature of the target for the formation of the experimental (Λp) effective mass spectrum.

In order to explain the nature of these peaks, the $\frac{F-B}{F+B}$ and $\frac{P-E}{P+E}$ ratios as a function of $M_{\Lambda p}$ for the angular distribution in the Λp -rest system were measured for one-proton events. These ratios are defined as in the Λp elastic scattering. The results are shown in fig. 3. The errors are statistical only.

In the region of the first (2058 MeV) peak both ratios are very near to zero. This fact strongly supports that the orbital angular momentum state is $1 = 0$ (S -state) and together with the small $Q_{\Lambda p} = M_{\Lambda p} - (M_\Lambda + M_p)$ value permitted us to apply to the Λp system the Watson theory of strong interactions in the final state.

Assuming the equality of the singlet and triplet state contributions and taking into account the background computed in the impulse approximation the (Λp) scattering length and the effective range were found to be equal to

$$a_{\Lambda p} = -(2.0 \pm 0.6) \times 10^{-13} \text{ cm}$$

$$r_{\Lambda p} = (2.5 \pm 0.8) \times 10^{-13} \text{ cm}$$

which are in fair agreement with the low energy Λp elastic scattering data /3/.

The negative sign of the $a_{\Lambda p}$ excludes the Λp bound states and explains the unsuccessfulness of Λ -hyperdeuteron searches.

The mass of the second peak (2127 MeV) is very near the ΣN threshold. This peak is probably due to the Σ -hyperon creation strongly interacting in the final state with a proton in the carbon nucleus with the further conversions in a Λ -hyperon via the $\Sigma N \to \Lambda p$ process.

This interpretation is strongly supported by the absence of asymmetries in Λ angular distributions (Fig. 3).

Finally, asymmetries were observed in the 2252 MeV mass peak region. Both $\frac{F-B}{F+B}$ and $\frac{P-E}{P+E}$ ratios are slowly raising from the ΣN threshold. The first ratio remains nearly constant, whereas the second ratio is slowly decreasing in the

region after the peak. Such a behaviour of the ratios probably indicates the existence of polarization effects in the (Λp) system near the 2252 MeV mass region. These facts permit one to suppose the existence of (Λp) resonance of the mass $M_{\Lambda p} = 2252$ and $\Gamma/2 \leq 15$ MeV half-width.

Next, the dibaryonic system of $S = 0$, namely the pp system obtained under the same experimental conditions was investigated.

In the neutron exposure from 6322 three-prong events 230 with two identified protons failed to satisfy the $np \to pp\pi^-(m\pi^0)$, $m = 0, 1, 2 \ldots$ channel fits. So we could conclude that these nonstrange dibaryonic proton-like events in $n\,{}^{1}_{0}\,C^{12}_{6}$ peripherical collisions were produced.

The corresponding pp effective mass spectrum is plotted in Fig. 10 (10 MeV bins).

In contrast to the strange proton-like (Λp) effective mass spectrum no enhancements are seen.

No enhancements are seen in the pp effective mass spectrum of two-proton carbon -like interactions (Fig. 1b, 4419 events).

The same situation repeats with two-proton $\pi^- C^{12}_{6} \to pp \ldots\ldots$ interactions (857 events, Fig. 2).

The form of the pp effective mass spectrum remained uncharged when a cut on the proton momenta 213 MeV/C $< P_{p_1}$, $P_{p_2} \leq 350$ Mev/C was imposed.

Our experiments could not reveal the peak due to the final state pp strong interaction because the maximum of this peak is situated at $Q_{pp} = 66$ KeV, whereas the pp mass resolution in the initial part of the spectrum was 2 MeV (stopping protons).

Contrary to this the Λp mass resolution of 3 MeV (stopping protons and slow Λ) for the initial part of the Λp effective

mass spectrum permitted us to observe the peak at $M_{\Lambda p} = 2058$ MeV ($Q_{\Lambda p} = 4.5$ MeV) corresponding to the strong Λp interaction in the final state.

2. $B = 2$; $S = -2$ System.

A search for $\Lambda\Lambda$ pairs in both exposures was performed. Fifty such pairs were identified altogether (30and 20 in neutron and pion exposures, respectively).

The ($\Lambda\Lambda$) effective mass spectrum is shown in Fig. 4. An analysis of possible processes leading to the pair formation permitted one to conclude that the $\Xi N \to 2\Lambda$ conversion process can account for only a very small part of the observed statistics (1%) because of small production and conversion cross sections. The observed opening angle distribution is forward-peaked, whereas for the conversion process it must prefer larger angles.

The $\Lambda\Lambda$ pair creation in the nuclear cascade process, when the second Λ is created by secondaries, especially by pions together with all other processes could give no more than 50% contribution.

We tried to imitate the ($\Lambda\Lambda$) effective mass spectrum by modelling the pair production in the nuclear cascade process. For this purpose we selected in the pion and neutron exposure statistics 50 pairs from different one- Λ events in such a way that the momenta and cosine of the emission polar angle of each coincided within 10 MeV/c and 0.05 respectively with those for the components of the really observed $\Lambda\Lambda$ pairs. The corresponding experimental and modelled P_Λ and $\cos\theta_\Lambda$ distributions are compared in Fig. 4. The differences in these distributions are clearly seen to be insignificant. Thus, the modelled pairs differ

from the real ones by only one parameter - the relative azimuthal ($\Lambda\Lambda$) angle.

The effective mass spectrum of the modelled $\Lambda\Lambda$ pairs normalized to 50% of the total weight of the observed $\Lambda\Lambda$ pairs by a dotted hystogram is shown (Fig. 4).

No consistence is found. The opening angle distrubution for modelled events is sharper than for the observed ones.

No consistence was found for the summary phase space volume distribution for the reactions

$$\pi^- {}_6C_6^{12} \to 2\Lambda 2K(mp)(ln)\left(\begin{matrix}A\\Z\end{matrix}\right)s\pi$$

$$n_0^1 \; {}_6C_6^{12} \to 2\Lambda 2K(mp)(ln)\left(\begin{matrix}A\\Z\end{matrix}\right)s\pi \qquad m, l, s = 0,1,2,\ldots$$

though to imitate the concentration of events in the first seven 30 MeV bins, we prescribed to each channel a weight equal to one.

On the other hand, neither of peaks observed earlier in the (Λp) mass spectrum is present in the corresponding (Λp) mass spectrum for 50 $\Lambda\Lambda$ observed pairs (131 combinations, Fig. 5).

This circumstance indicates that the enhancement in the (2231 ÷ 2381) MeV region of the $\Lambda\Lambda$ effective mass spectrum is not due to known Λp enhacements in the Λp effective mass spectrum.

All these facts, in our opinion, may support the possibility of the $\Lambda\Lambda$ creation in the primary interaction of the incident particles with nuclear substructures.

The enhancement in the (2231 ÷ 2381) MeV may be due to a resonance in the $\Lambda\Lambda$ -system.

An alternative cause of the concentration of $\Lambda\Lambda$ pairs in the mass region (2231 ÷ 2381)MeV can be due to the strong $\Lambda\Lambda$ interaction in the final state.

An analysis within the frame of the Watson theory, taking as a background the phase space volume distribution, was performed. The minimum of the χ^2_2 dependence on the $\Lambda\Lambda$ scattering length and effective range clearly prefers (Fig. 4).

$$-1.0 \times 10^{-13}\ cm < a_{\Lambda\Lambda} < 0$$

$$1.5 \times 10^{-13} cm < r_{\Lambda\Lambda} < 3.0 \times 10^{-13}\ cm$$

in agreement with the double hyperfragment data /4/.

3. $B = 3$; $S = -1$ System.

The effective mass spectrum of the ($pp\Lambda$) system from 742 events containing a Λ and (2 ÷ 5) protons is presented in Fig. 6. No significant peaks are seen. An analysis showed that irregularities contain the events for which $M_{\Lambda p}$ combinations fall in the peak regions observed at 2058, 2127 and 2252 MeV.

Conclusions.

Two independent experiments were performed, and the following results were obtained.

1. In the Λp ($B = 2$, $Y = 1$, $S = -1$) effective mass spectrum significant peaks at 2058, 2127 and 2252 MeV values were observed. The first and the second peaks are due to the strong Λp and ΣN final state interactions, respectively, with the subsequent $\Sigma N \to \Lambda p$ conversion.

The Λp scattering lengths and effective radius being in good agreement with the low energy Λp elastic scattering result were defined.

The peak at the 2252 MeV mass value most probably is due to a (Λp) resonance of $\Gamma/2 \leq 15$ MeV half-width.

2. In the (pp) system effective mass spectrum no enhacement were observed.

3. In the ($\Lambda\Lambda$) ($B = 2$, $Y = 0$, $S = -2$) effective mass spectrum an enhacement in the (2231 ÷ 2381) MeV region of the spectrum with respect to the phase space volume was observed.

The enhacement may be due to ($\Lambda\Lambda$) resonance. Alternatively the above-mentioned concentration may be explained by the strong final state interaction. The $\Lambda\Lambda$ scattering length and the effective radius deduced in the frame of the Watson theory agree with the result obtained in the double hyperfragment experiment.

This alternative possibility may be significant if the validity of the Watson theory is supposed for the region of $Q_{\Lambda\Lambda}$ used.

4. In the ($pp\Lambda$) ($B = 3$, $Y = 2$, $S = -1$) effective mass spectrum no significant enhacements are observed. The irregularities observed may be explained by kinematical reflections of the peaks from the (Λp) mass spectrum.

The authors are very much indepted to A.U. Sokovnina, M.A. Prislonova, M.I. Phillipova, L.U. Bannik, L.A. Martinova and H.A. Kalinina and express their deep gratitude for the help.

Sincere aknowledgements are due to Yu.A. Troyan, A.P. Gasparyan and A.V. Nikitin for the permission to use their 230 non-strange proton-like events.

Sincere aknowledgements are due to V.A. Beliakov for his help in programming work.

References

1. B.A. Shahbazian. Voprosy Fiziki Elementarnykh Chastits 543, v. 4, Erevan (1964).

2. B.A. Shahbazian and V.I. Moroz. JINR, E1-4022, Dubna (1968); JETP Pis'ma, v. 5, 307 (1967); JINR, P1-3169, Dubna (1967); High Energy Physics and Nuclear Structure 524, Plenum-press, N.Y.-London, 1970.
3. G. Alexander et al., Phys. Rev., 173, 1452 (1968).
4. S. Ali and A.R. Bodmer. Int. Atomic Energy Agency. Int. Centre for Theor. Phys., 1c/66/112, 1966. Piazza Oberdan Trieste.

Received by Publishing Department
on July 15, 1971.

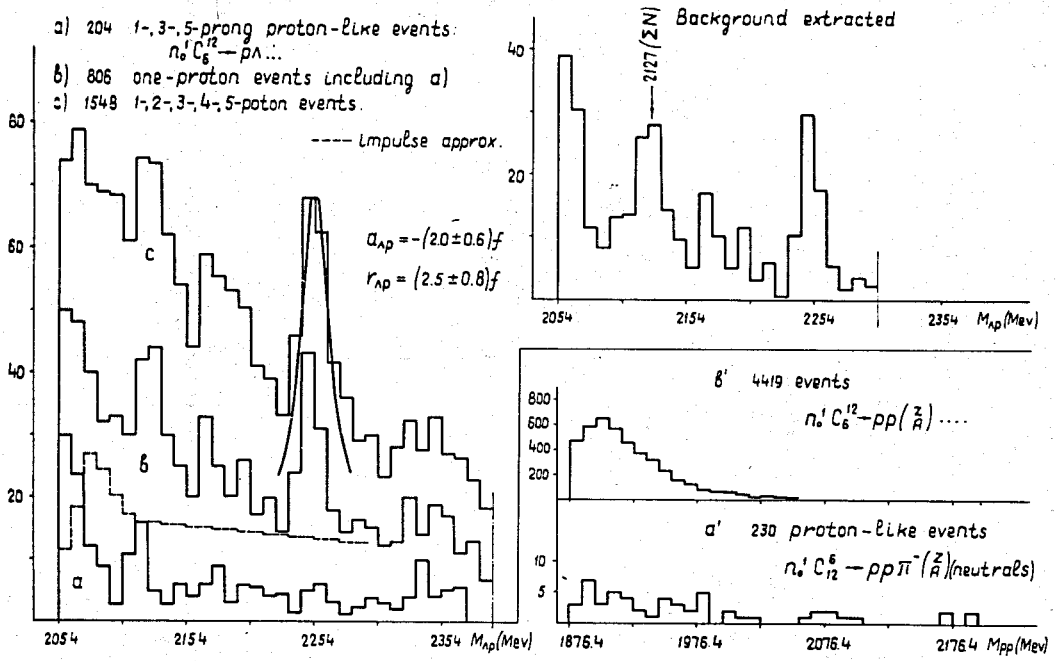

Fig. 1. The neutron exposure $\langle p_n \rangle$ = 7.5 GeV/c. The (Λp) effective mass spectrum for a) 204 1-, 3-, 5- prong proton-like events; b) 806 one-proton events including a); c) 1548 Λ and (1 ÷ 5)- proton events with the contribution of each sample of n_p-proton multiplicity weighted by $1/n_p$ (normalized to N_Λ^{tot} = = 1548); the effective mass resolution function by the solid line curve is shown. The (Λp) effective mass spectrum for b) with background extracted. The (pp) effective mass spectra for a) 230 proton-like events; b) 4419 two-proton events.

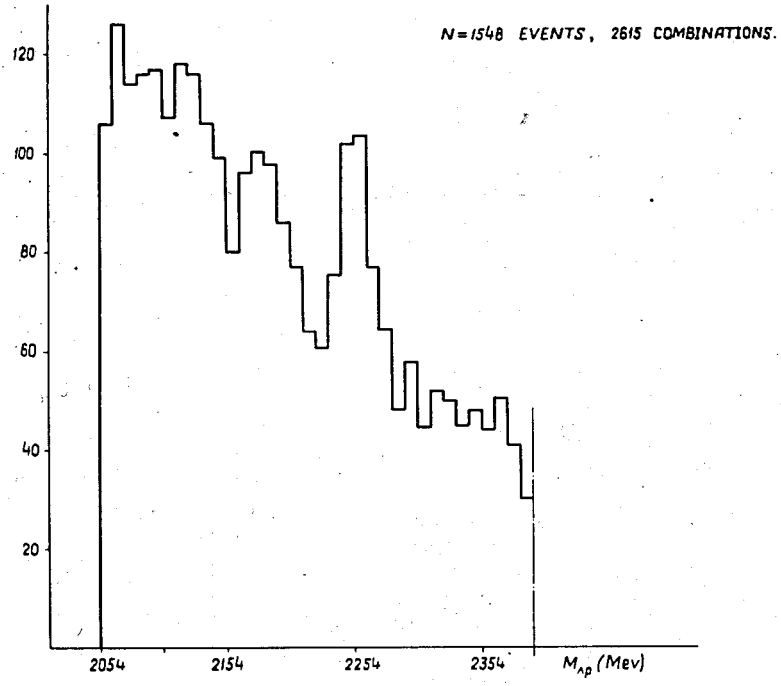

Fig. 1d. The (Λp) effective mass spectrum for all 2615 combinations from 1548 events.

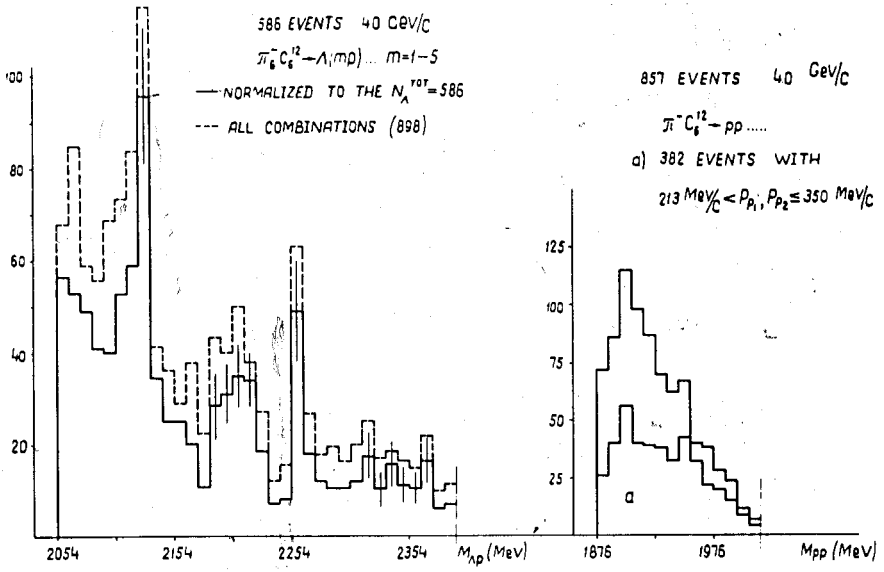

Fig. 2. The π^--exposure at 4.0 GeV/c. The (Λp) effective mass spectrum for 586 Λ and (1 ÷ 5)-proton events normalized to N_Λ^{tot} = 586 (the solid-line hystogram). The same for all 898 (Λp) combinations. M_{pp} for 857 two-proton events; a) the same with the cut 213 MeV/c $< p_{p_1}$, $p_{p_2} \leq$ 350 MeV/C imposed on the proton momenta.

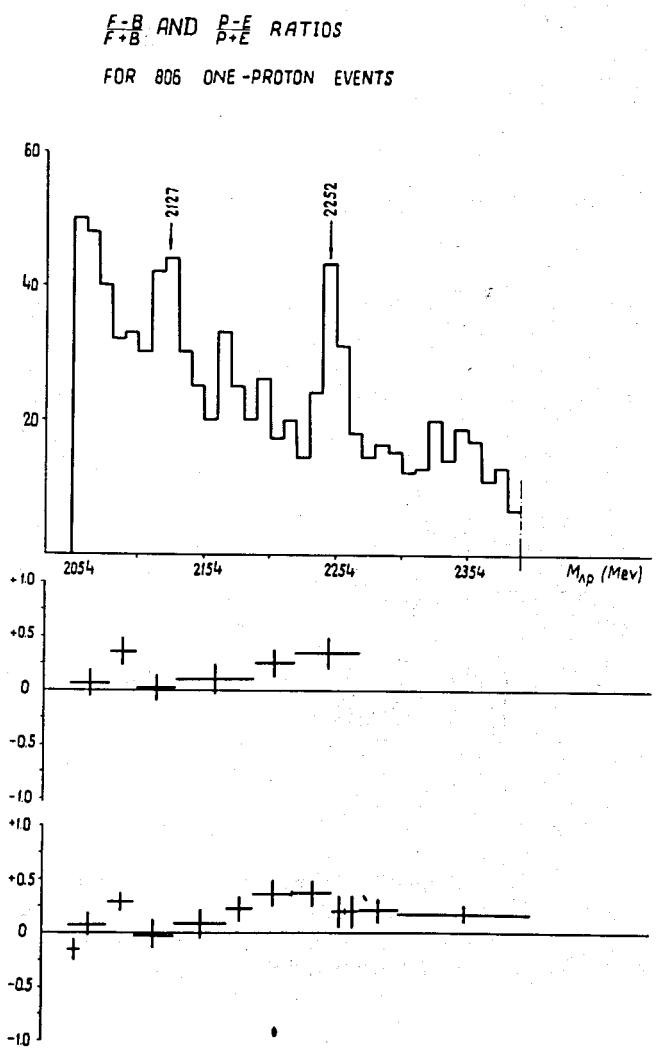

Fig. 3. $\frac{F-B}{F+B}$ and $\frac{P-E}{P+E}$ ratios as functions of the (Λp) effective mass.

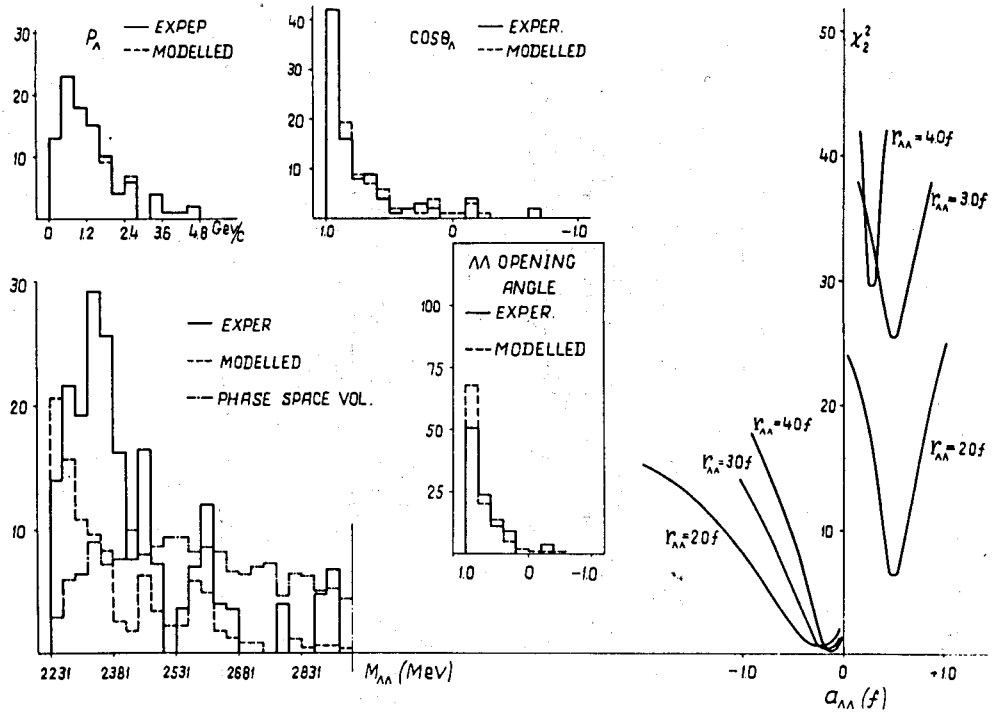

Fig. 4. The 50 ($\Lambda\Lambda$) pairs effective mass spectrum. The Λ momentum, polar angle and ($\Lambda\Lambda$) opening angle distributions for the real and modelled $\Lambda\Lambda$ pairs. The dependence of χ^2_2 on positive and negative $\Lambda\Lambda$ scattering length $a_{\Lambda\Lambda}$ ($r_{\Lambda\Lambda}$ as a parameter).

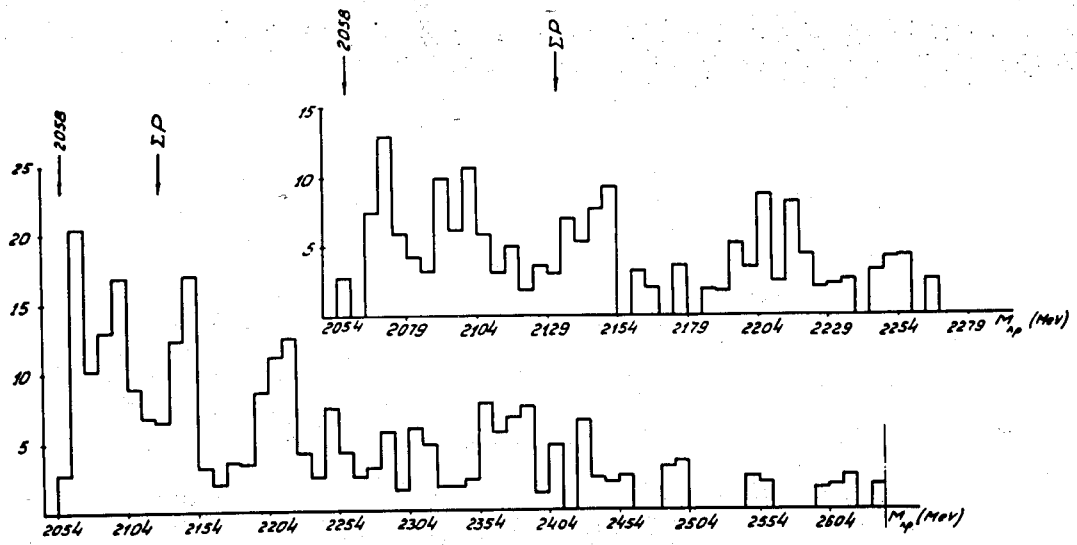

Fig. 5. The (Λp) effective mass spectrum for 50 $\Lambda\Lambda$ events (131 Λp combinations).

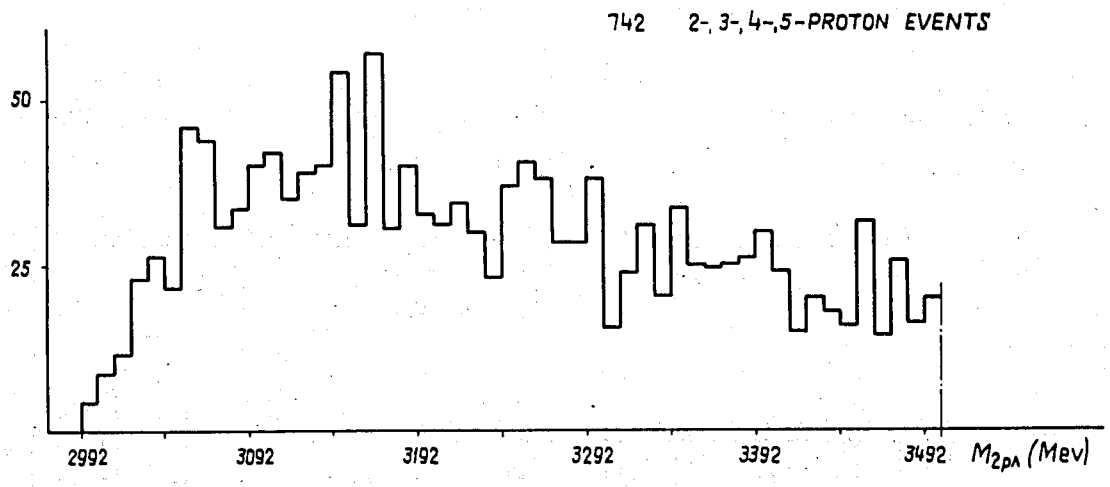

Fig. 6. The (Λpp) effective mass spectrum for the neutron exposure (742 events).